

Three-Dimensional Vortex Theory of Axial Compressor Blade Rows at Subsonic and Transonic Speeds

OLUFEMI OKUROUTUMU* AND JAMES E. MCCUNE†

Massachusetts Institute of Technology, Cambridge, Mass.

The three-dimensional, inviscid, small-perturbation, compressible flow past a lifting axial compressor rotor is analyzed. Because of its three-dimensional nature the solution applies for transonic as well as subsonic relative speeds. A potential solution is constructed, representing B lifting blades each with bound vorticity of total strength $\Gamma(r)$. If $\Gamma(r)$ is nonuniform, vorticity is shed downstream, which in turn induces a modified flowfield at the rotor. In addition, for supersonic relative tip Mach numbers, acoustic radiation occurs. Both of these effects introduce drag at the blades. Given $\Gamma(r)$, or the mean change in circumferential velocity, the first-order static and total pressure rise, axial velocity change, etc., are determined. A second-order calculation yields the power required, including the effects of induced and wave-drag. An ideal efficiency is defined which indicates the penalty associated with departure from constant work design, as well as with losses due to acoustic radiation. For a 20% variation of Γ across the blade span, the combination of both types of losses for a typical, but lightly-loaded, transonic rotor are of the order of 0.5%.

Nomenclature

a	= unperturbed speed of sound, far upstream of rotor, $a^2 \equiv \gamma[(p)_{-\infty}/\sigma_{-\infty}]$	r	= radial coordinate
A_{nk}	= coefficients of eigenfunctions	r_H, r_T	= hub radius, tip radius
B	= number of blades	$R_{nB}(K_{nk}\eta)$	= orthonormal radial eigenfunctions = $(M_{nBk})^{-1} \{J_{nB}(K_{nk}\eta) - [\gamma_{nk}/(3)^{1/2}]N_{nB}(K_{nk}\eta)\}$
$c(r), c_{ax}$	= local blade chord, axial projection of local chord	t	= time variable
C	= $\frac{2}{1 - h^2} \int_h^1 \eta d\eta \Gamma(\eta)$	T	= torque required by rotor
$F_\theta(r), F_z(r)$	= circumferential and axial components of force on blade at each section	U	= unperturbed axial speed, far upstream of rotor
h	= hub-to-tip ratio, r_H/r_T	U_r	= unperturbed relative speed, far upstream of rotor, $U_r^2 = U^2(1 + \rho^2)$
$h(r, \theta, x)$	= static enthalpy	u	= axial perturbation velocity, $u = \partial\phi/\partial x$
H_d, H_r	= total enthalpy in duct coordinates, rotor coordinates	v	= circumferential perturbation velocity, $v = (1/r) \partial\phi/\partial\theta$
$I_n(x)$	= modified Bessel function of first kind, order n	v_r	= radial velocity component
$J_n(x)$	= Bessel function of first kind, order n	\dot{W}	= rate of work done by rotor
k	= index	x, z	= axial coordinate (rotor or duct coordinates); $z \equiv \omega x/U$
$K_n(x)$	= modified Bessel function of second kind, order n	$Z(\rho_T, \rho_H)$	= defined below Eq. (5)
K_{nk}	= radial eigenvalues	β	= $(1 - M^2)^{1/2}$
$L(r)$	= lift per blade at each section	γ	= ratio of specific heats
L_T	= blade spacing at the tips, $L_T = 2\pi r_T/B$	$\Gamma(r)$	= blade circulation at each section
M	= axial mach number of undisturbed flow, $M = U/a$	δ	= mean turning angle viewed in rotor coordinates
M_r	= unperturbed relative Mach number at each section, $M_r^2 = [U^2/a^2](1 + \omega^2 r^2/U^2)$	ζ	= helical variable, $\theta - z$
M_{rT}	= M_r evaluated $r = r_T$	η	= dimensionless radius, r/r_T
n	= index	θ	= circumferential coordinate, rotor coordinates
$N_n(x)$	= Neumann function, order n	λ_{nk}	= eigenvalue for axial eigenfunctions, Eq. (7)
$p, (p)_{-\infty}$	= pressure perturbation, reference static pressure	μ_{nk}	= $-i\lambda_{nk}$
p_0	= total pressure, duct coordinates	ρ	= dimensionless radial coordinate, $\omega r/U$
$(p_0)_{-\infty}$	= reference total pressure, duct coordinates	σ	= perturbation mass density
		$\sigma_{-\infty}$	= reference mass density, far upstream of rotor
		$\phi(z, \theta, \rho)$	= perturbation velocity potential, rotor coordinates
		$\phi(\rho)$	= $\tan\rho^{-1}$, complement of local stagger angle
		$\chi_n(\rho)$	= $\chi_{nB}(nB\rho)$, see Eqs. (4) and (5)
		ω	= angular speed of rotor

Received June 3, 1969; revision received October 6, 1969. A major portion of this work is contained in the Sc.D. thesis, Department of Mechanical Engineering, Massachusetts Institute of Technology of O. Okurounmu who subsequently joined the United Aircraft Research Laboratories as a Research Engineer. Both authors wish to express their appreciation for the hospitality of the United Aircraft Research Laboratories where many of the numerical results presented here were obtained, and where a portion of the present manuscript was written. Many useful conversations with members of the Research Laboratories Staff and of the Compressor Group at Pratt and Whitney Aircraft are gratefully acknowledged.

* Research Assistant, Department of Mechanical Engineering; now member of the faculty, University of Lagos, Lagos, Nigeria.

† Professor, Department of Aeronautics and Astronautics; Consultant, United Aircraft Research Laboratories, East Hartford, Conn.

Superscripts

u, d	= upstream, downstream of rotor
w	= quantity associated with wakes (Reisner) potential
(1), (2)	= first- and second-order results, respectively

Subscripts

$-\infty$	= indicates quantity far upstream of rotor, or a reference quantity when acoustic radiation is present
∞	= indicates quantity evaluated as $z \rightarrow +\infty$
l	= index indicating change in cyclic constant across wakes
i	= quantity "induced" by wake flow when $\Gamma \neq \text{const}$
r, d	= rotor and duct coordinates, respectively

w = quantity associated with acoustic radiation
 ρ, θ, z, ζ = partial differentiation with respect to ρ , etc., as indicated

Special notation

$\langle \rangle$ = circumferential average
 $\Delta()$ = $[()^d - ()^u]_{z=0}$
 $()'$ = prime denotes differentiation with respect to argument, except as noted below Eq. (5)
 $\ll \gg$ = average over flow annulus

I. Introduction

IN the following, the basic three-dimensional solution for the linearized compressible potential flow through a lifting axial compressor rotor is developed. Because of its three-dimensional nature the solution can be applied for subsonic, transonic, and supersonic relative Mach numbers at the rotor tip. In the present paper the axial Mach number is assumed less than unity, corresponding to situations of current major interest; however, the method can be modified easily to treat the problem with supersonic axial flow if desired.

In Sec. II, the elementary (Green's function) solution of the potential equation for a lifting rotor in compressible flow is obtained, representing B bound vortex lines of strength $\Gamma(r)$, rotating at constant speed in an annular duct of infinite axial extent. The undisturbed velocity far upstream of the rotor is assumed subsonic and purely axial. When $\Gamma(r)$ is not a constant ("constant work" design) free vorticity is necessarily shed downstream of the rotor blades, with a strength proportional to $d\Gamma/dr$. In the linearized approximation, this leads to a set of B helical vortex sheets (viewed in the rotating coordinate system fixed in the rotor blades) trailing downstream of the rotor with speed $(U^2 + \omega^2 r^2)^{1/2} \equiv U_r$. In rotor coordinates the flow is steady.

The aforementioned trailing vortex sheets induce a velocity field that modifies the flow seen by the rotor. In addition, of course, each of the bound vortex lines (or blades—see below) affects the flow as seen by each of its neighbors. In analogy with the usual wing theory, an "induced drag" results from the trailing helical sheets ("wakes") of shed vorticity, and this modifies the power required to drive the rotor (Sec. IV).

For many purposes, the flow upstream and downstream of the rotor is not particularly sensitive to the details of the chordwise loading or camber. In this case we may simply regard $\Gamma(r)$ of the elementary solution itself as the local chordwise integral of the distributed bound vorticity representing the blades (i.e., the blade circulation). We adopt this approach in Sec. III. For example, $\Gamma(r)$ exactly specifies the mean swirl induced by the rotor, independent of the chordwise loading. Using this point of view, we develop in Sec. III certain "integral relationships" between $\Gamma(r)$ (or the turning angles) and the first-order static and total pressure rise produced by the rotor, as well as the first-order torque required.

In Sec. IV we extend the results of the linear theory by computing the required rotor power correct to second order in first-order quantities. The results enable us to define an "ideal efficiency," indicating the power loss associated with nonuniform Γ (departure from "constant work" design) as well as that due to acoustic radiation when the relative tip Mach number is supersonic. (To obtain the latter result we must allow a finite chord for the blades, i.e., the bound vorticity must be distributed over finite helical surfaces as in the lifting surface theory, the development of which will be reported later. For this purpose we use here an elementary version of the latter theory in which the distributed vorticity is given by $\Gamma(r)/c(r)$, where $c(r)$ is the local chord of the blades.)

Although our basic theory is in fact an isentropic one, we are able to define the aforementioned "ideal efficiency" by

reference to an "equivalent constant work state" defined as that corresponding to a uniformly loaded rotor with the same mean loading as the actual rotor. The definition of the ideal efficiency is discussed more completely in Sec. IVa.

We recognize, of course, that the over-all efficiency loss—and/or increase in drag—in axial compressor stages is largely attributable to a combination of viscous and nonlinear compressibility effects not included in the present theory. It is our hope here, however, to indicate what portion of efficiency decrement may occur in a compressor even in the absence of viscous effects, particularly as one departs from design-point operation.

Numerical results for the ideal efficiency are presented and discussed in Sec. V.

Our first task in analyzing the flow through the blade row is a study of the wakes of shed vorticity which will arise if $\Gamma \neq \text{const}$. Far downstream of the rotor, helical symmetry of the flow will develop (except for acoustic radiation when the rotor tip Mach number is supersonic) and this helical flow becomes effectively incompressible. Reissner¹ analyzed the incompressible flow through a screw propeller in free air by constructing a solution for the velocity potential across the trailing helical sheets. Reissner's method was later adapted by Davidson² in an attempt to obtain the solution for the compressible flow through a ducted propeller. The present study is a further adaptation of Reissner's work, with application to a compressor or a ducted fan. Compressibility effects are included by adding to the far-wake solution a complete set of eigensolutions of the full potential equation and applying appropriate matching conditions at the rotor plane. An error which considerably limits the usefulness of Davidson's study is removed in the present analysis.

The result can be viewed as the "lifting part" of the complete (linearized) theory of inviscid flow through an axial compressor blade row. The "thickness problem" was worked out earlier.³

II. Formulation of the Problem

If we consider a blade row advancing through still air with axial speed U and rotating with angular velocity ω , and let $(x_1, r_1, \theta_1, t_1)$ be coordinates fixed in space, then the linearized disturbance field produced by the blades satisfies the wave equation. In terms of the velocity potential $\phi_1(x_1, r_1, \theta_1, t_1)$ we have

$$\nabla_1^2 \phi_1 = (1/a^2) \partial^2 \phi_1 / \partial t_1^2 \quad (1)$$

It is here assumed that in the regions of interest the flow is inviscid and irrotational, being due to small perturbations caused by the rotor. If we transform into coordinates (x, r, θ) , which advance and rotate with the blades, then the flow will be steady as viewed from these coordinates. Thus, the transformations to "rotor coordinates," $x = x_1 + U t_1$, $r = r_1$, $\theta = \theta_1 + \omega t_1$, yield $\phi_1(x_1, r_1, \theta_1, t_1) = \phi(x, r, \theta)$. The geometry is illustrated in Fig. 1. Further, if we introduce the parameters $M = U/a$ and $\beta^2 = 1 - M^2$ and the dimensionless coordinates $z = \omega x/U$, $\rho = \omega r/U$, Eq. (1) can be expressed as

$$\beta^2 \phi_{zz} + \phi_{\rho\rho} + (1/\rho) \phi_\rho + (1/\rho^2)(1 - M^2 \rho^2) \phi_{\theta\theta} - 2M^2 \phi_{z\theta} = 0 \quad (2)$$

Eq. (2) can also be written using the helical coordinate $\zeta \equiv \theta - z$, with $\phi(z, \rho, \theta) = \varphi(z, \rho, \zeta)$,

$$\beta^2 \varphi_{zz} + \varphi_{\rho\rho} + (1/\rho) \varphi_\rho + (1 + 1/\rho^2) \varphi_{\zeta\zeta} - 2\varphi_{\zeta z} = 0 \quad (2a)$$

The boundary conditions on Eq. (2) or Eq. (2a) for the present problem are that ϕ change discontinuously across the trailing helical vortex sheets emanating from the blades, such that the change across each sheet is equal to the total

bound circulation $\Gamma(\rho)$. In addition, the potential must be bounded at infinity, whereas the radial velocities must vanish at the bounding walls. If acoustic radiation occurs, it must be directed away from the rotor, both upstream and downstream.

A. Wake Solution

Equation (2a) reduces in the far wake, (analogous to the Trefftz plane) to

$$(1/\rho)(\rho\varphi_\rho)_\rho + (1 + 1/\rho^2)\varphi_{\zeta\zeta} = 0 \quad (3)$$

Equation (3) is independent of Mach number and is in fact simply Laplace's equation, expressed in the coordinates ρ and ζ ; hence, its formal solution must be similar to Reissner's, the difference being the presence, in this case, of bounding walls at the hub and shroud. Taking the latter into account, we obtain a Reissner type solution to Eq. (3), satisfying the aforementioned boundary conditions in the form

$$\phi^{(w)} = \frac{B}{2\pi} \left[\Gamma(\rho)\zeta_i + \sum_{n=1}^{\infty} \frac{(-2)(-1)^n}{nB} \chi_n(\rho) \sin(nB\zeta) \right] \quad (4)$$

where

$$\begin{aligned} \chi_n(\rho) \equiv \chi_{nB}(nB\rho) = & \frac{K'(\rho_T)I'(\rho_H)K(\rho) - K'(\rho_T)K'(\rho_H)I(\rho)}{Z(\rho_H, \rho_T)} \int_{\rho_H}^{\rho_T} \xi d\xi I'(\xi) \frac{d\Gamma}{d\xi} + \\ & \frac{I'(\rho_T)K'(\rho_H)I(\rho) - I'(\rho_H)I'(\rho_T)K(\rho)}{Z(\rho_H, \rho_T)} \int_{\rho_H}^{\rho_T} \xi d\xi K'(\xi) \frac{d\Gamma}{d\xi} + \\ & I(\rho) \int_{\rho_H}^{\rho} K'(\xi) \xi \frac{d\Gamma}{d\xi} d\xi - K(\rho) \int_{\rho_H}^{\rho} I'(\xi) \xi \frac{d\Gamma}{d\xi} d\xi \quad (5) \end{aligned}$$

Here, $I(\rho)$, $I'(\rho)$, $K(\rho)$, $K'(\rho)$ are the modified Bessel functions of the first and second kind, and their derivatives. We have adopted the shorthand notation

$$K'(\rho) \equiv (d/d\rho)K_{nB}(nB\rho); K(\rho) \equiv K_{nB}(nB\rho), \text{ etc.}$$

and

$$Z(\rho_H, \rho_T) \equiv K'(\rho_T)I'(\rho_H) - K'(\rho_H)I'(\rho_T)$$

In obtaining the form of Eq. (5) for the functions $\chi_n(\rho)$ we have made frequent use of the Wronskian

$$I_n(x)(d/dx)K_n(x) - K_n(x)(d/dx)I_n(x) = -1/x$$

and have integrated once by parts in each of the integrals. In this form one sees immediately that each χ_n vanishes if $\Gamma = \text{const.}$ The wake solution Eq. (4) satisfies the boundary conditions at the walls whether or not $d\Gamma/dr = 0$ at r_H and r_T .

The function ζ_i appearing in Eq. (4) is a periodic ("saw-tooth") function that varies linearly with ζ between the blades, but changes discontinuously (by an amount $2\pi/B$) across each blade—or its associated trailing vortex sheet for $z > 0$ —as described in Ref. 1.

In interpreting this discontinuous part of the wake potential, it is helpful to recall that it is intended to represent the discontinuity in potential across the wakes of free vorticity trailing behind the blades; thus only the radial component of velocity ($\partial\phi/\partial r$) is discontinuous at the wakes (with discontinuity proportional to $d\Gamma/dr$) while $u = \partial\phi/\partial x$ and $rv = \partial\phi/\partial\theta$ are continuous there. Hence we must take $\partial\zeta_i/\partial\theta = 1$, $\partial\zeta_i/\partial z = -1$. The index l simply indicates the change in cyclic constant associated with ϕ in each successive sector between the blades or their associated wakes.

B. Complete Solution

The complete solution to Eq. (2) is obtained by adding to the wake solution a complete set of eigensolutions of Eq. (2), in such a manner that the combined solution satisfies the re-

quired boundary conditions and the additional physical requirements of continuity of mass flow at $z = 0$. We begin by noting some obvious special solutions of Eq. (2)

$$\phi^{[1]} = Cz, \phi^{[2]} = D\theta, \phi^{[3]} = K\zeta$$

Of these, only the first ($\phi^{[1]}$) will be needed; indeed, its inclusion in the downstream flowfield is essential for mass conservation. This vital fact was overlooked in Ref. 2.

If we now look for solutions of Eq. (2) proportional to $\exp(inB\theta)$ we find the additional doubly-infinite set of eigen-solutions

$$\phi_{nk}^{u,d} = A_{nk}^{u,d} \exp(inB\theta) \exp[(inBM^2/\beta^2 \pm \lambda_{nk})z] \times R_{nB}(K_{nk}\rho/\rho_T) \quad (6)$$

where

$$\lambda_{nk} = (1/\beta)(K_{nk}^2/\rho_T^2 - n^2B^2M^2/\beta^2)^{1/2} \quad (7)$$

The cylinder functions $R_{nB}(K_{nk}\rho/\rho_T)$ are normalized, linear combinations of Bessel and Neumann functions, and their properties are fully described in Refs. 3 and 4. The coefficients $A_{nk}^{u,d}$, for regions upstream and downstream of $z = 0$, are determined by the matching conditions described below. The eigenvalues K_{nk} are such that $R_{nB}'(K_{nk}) = R_{nB}'(hK_{nk}) = 0$. The sign of λ_{nk} in Eq. (7) is chosen so that when λ_{nk} is real, the perturbations die out at large distances upstream and downstream from the rotor, while for imaginary values of λ_{nk} , the propagating disturbances have a higher pitch upstream than downstream.⁴ Thus,

$$\begin{aligned} \phi^u &= \sum_{n=1}^{\infty} \sum_{k=1}^{\infty} \phi_{nk}^u + \sum_{k=1}^{\infty} \phi_{0k}^u \\ \phi^d &= \sum_{n=1}^{\infty} \sum_{k=1}^{\infty} \phi_{nk}^d + \sum_{k=1}^{\infty} \phi_{0k}^d + \phi^{[1]} + \phi^{[w]} \end{aligned}$$

The coefficients $A_{nk}^{u,d}$ and C occurring in these expressions are determined by the matching conditions at the plane $z = 0$ corresponding to the lifting problem, namely that ϕ be continuous everywhere on this plane except at the blades, and no additional mass be introduced there. The result is (real part implied)

$$\begin{aligned} \phi^u &= \frac{B}{2\pi\beta^2} \left\{ \sum_{k=1}^{\infty} \left(-\frac{\Gamma_{0k}}{2\lambda_{0k}} \right) e^{\lambda_{0k}z} R_{0B}(K_{0k}\eta) + \right. \\ & \sum_{n=1}^{\infty} \sum_{k=1}^{\infty} \left[\frac{i\beta^2(-1)^n}{nB} (\Gamma_{nk} + h_{nk}) + (-1)^n \frac{h_{nk}}{\lambda_{nk}} \right] \times \\ & e^{inB\theta} \exp \left[\left(\frac{inBM^2}{\beta^2} + \lambda_{nk} \right) z \right] R_{nB}(K_{nk}\eta) \Big\}; z < 0 \\ \phi^d &= \frac{B}{2\pi\beta^2} \left\{ Cz + \beta^2\Gamma(\eta)\zeta_i + \sum_{k=1}^{\infty} - \right. \\ & \left(\frac{\Gamma_{0k}}{2\lambda_{0k}} \right) e^{-\lambda_{0k}z} R_{0B}(K_{0k}\eta) + \\ & \beta^2 \sum_{n=1}^{\infty} \sum_{k=1}^{\infty} \frac{(-1)^n 2i}{nB} h_{nk} e^{inB\theta} R_{nB}(K_{nk}\eta) + \\ & \sum_{n=1}^{\infty} \sum_{k=1}^{\infty} \left[\frac{-i\beta^2(-1)^n}{nB} (\Gamma_{nk} + h_{nk}) + (-1)^n \frac{h_{nk}}{\lambda_{nk}} \right] \times \\ & e^{inB\theta} \exp \left[\left(\frac{inBM^2}{\beta^2} - \lambda_{nk} \right) z \right] R_{nB}(K_{nk}\eta) \Big\}; z > 0 \quad (8) \end{aligned}$$

The coefficients C , Γ_{nk} and h_{nk} occurring in the preceding are those resulting from expansions of the functions $\Gamma(\eta)$ and $\chi_n(\eta)$ in a series of the orthonormal functions $R_{nB}(K_{nk}\eta)$. Thus

$$h_{nk} = \int_h^1 \eta d\eta \chi_n(\eta) R_{nB}(K_{nk}\eta); n \geq 1$$

$$\Gamma_{nk} = \int_h^1 \eta d\eta \Gamma(\eta) R_{nB}(K_{nk}\eta); n \geq 0$$

$$C = \frac{2}{1 - h^2} \int_h^1 \eta d\eta \Gamma(\eta)$$

The necessity of the constant C (and hence the inclusion of $\phi^{(1)}$) follows from the fact that the R_0 's do not form a complete set.⁵ For example

$$\Gamma(\eta) = C + \sum_{k=1}^{\infty} \Gamma_{0k} R_0(K_{0k}\eta); n = 0$$

while

$$\Gamma(\eta) = \sum_{k=1}^{\infty} \Gamma_{nk} R_{nB}(K_{nk}\eta); n \geq 1$$

It will be seen that $\phi^{(1)}$ allows for a density change across the rotor.

Formally, these results are obtained using the orthonormality of the radial and azimuthal eigenfunctions and the fact that the local change in mass flow across the plane $z = 0$ is

$$\Delta \dot{m}(r, \theta) = \beta^2 \Delta u - (\omega M^2 / U) \Delta(rv)$$

Using the fact that ζ_l (θ_l for $z = 0$) has the Fourier expansion [valid everywhere except at $\zeta = (2l + 1)\pi/B$],

$$\zeta_l = \text{Re} \left[\sum_{n=1}^{\infty} \frac{(-1)^{n2i}}{nB} e^{inB\zeta} \right]$$

one can directly verify from Eq. (8) that $\Delta\phi = 0$ except at the bound vortices and that

$$r\Delta v = \frac{B\Gamma(\rho)}{2\pi} \left\{ 1 + \sum_{n=1}^{\infty} (-1)^{n2} \cos nB\theta \right\} = \Gamma(\rho) \sum_{l=-\infty}^{\infty} \delta\left(\theta_l - \frac{\pi}{B}\right)$$

We see that the integral across each lifting line of this quantity is just the circulation $\Gamma(\rho)$, since, as indicated, the middle expression is the Fourier representation of a periodic delta-function in θ , multiplied by $\Gamma(\rho)$, with singularities located at $\theta = \pm\pi/B, \pm 3\pi/B, \dots$

Before proceeding it is useful here to discuss a few additional features of our elementary solution. The quantities λ_{nk} [Eq. (7)] play a crucial role in determining the properties of the solution. If the flow in rotor coordinates is completely subsonic (subsonic relative Mach number at the rotor tip) all λ_{nk} 's are real and positive. It is evident from Eq. (7) that for imaginary λ_{nk} to occur we must have

$$\beta^2 / M^2 = \rho_s^2 < (n^2 B^2 / K_{nk}^2) \rho_T^2$$

where $\rho_s = \omega r_s / U$ is the dimensionless radius of the "sonic cylinder," i.e., the radial station at which $U^2 + \omega^2 r^2 = a^2$. However, it is well known⁶ that the (positive real) radial eigenvalues K_{nk} are all greater than $|nB|$, the order of the radial eigenfunctions. Hence, the preceding inequality would require $\rho_s < \rho_T$, i.e., it would imply that the relative Mach number at the tips is supersonic.

Thus, within the present theory imaginary λ_{nk} occurs only for $n > 0$ and $M_{rT} > 1$, and in such cases our solution indicates acoustic radiation upstream and downstream of the rotor with an associated increase in drag and noise.

We note that for each $n > 0$, only a finite number of the λ_{nk} 's can be imaginary; the K_{nk} 's increase monotonically with k so that even if $\rho_s < \rho_T$, eventually the preceding inequality cannot be satisfied. This leads to the definition of a k_n^* for each n : we denote by k_n^* the maximum value of the index k for any n such that λ_{nk} is imaginary. Clearly, $k_n^* = 0$ (for all n) if $M_{rT} < 1$.

If a given λ_{nk} is imaginary we replace it by

$$\lambda_{nk} = i\mu_{nk}$$

where the μ_{nk} 's, so defined, are real and positive.

C. Transonic Resonance

According to Eq. (7) it is also possible, if $M_{rT} > 1$, for one or more of the λ_{nk} 's ($n > 0$) to vanish. Returning to the solution, Eq. (8), we see that this leaves the coefficients undefined, unless $h_{nk} \equiv 0$ (see below). This is the "transonic resonance" effect which plays such an important role in the thickness problem.³ As pointed out in Ref. 3, the physical meaning of this resonance is that the corresponding upstream and downstream eigenmodes have a perfectly matched acoustic impedance at the rotor plane. In that case a steady-state amplitude of such modes cannot be achieved within the approximation of Eq. (1) if they are excited by the rotor.

To treat this situation, a slight modification of the theory is necessary. Either by including viscous effects, as in Ref. 3, or by including certain nonlinear terms, one is able to determine finite amplitudes for the resonant modes. We adopt the former technique in Sec. V; discussion of the effect of nonlinear terms will be given in a later paper.

We wish to point out here, however, that for the lifting problem the resonance is associated only with the coefficients h_{nk} , which vanish identically if $d\Gamma/dr = 0$. Hence, there is no transonic resonance for the lifting problem if $\Gamma = \text{const}$.

III. General First-Order Results

All flow quantities derivable from the solution Eq. (8) are known if the sectional circulation of the blades $\Gamma(r)$ is specified (the so-called "inverse" aerodynamic problem). We now use this solution to develop relationships between $\Gamma(r)$ and certain average flow properties of interest in compressor design.

Far downstream of the rotor the tangential velocity (viewed in rotor coordinates) becomes

$$v(r, \theta, z \rightarrow \infty) = \frac{B\Gamma(\rho)}{2\pi r} + \frac{B}{2\pi r} \sum_{n=1}^{\infty} (-2)(-1)^n \chi_n(\rho) \times \cos(nB\zeta) + \frac{B}{2\pi\beta^2} \sum_{n=1}^{\infty} \sum_{k=1}^{k_n^*} \left\{ \frac{(-1)^n n B h_{nk}}{\mu_{nk}} + \beta^2 (-1)^n \times (h_{nk} + \Gamma_{nk}) \right\} R_{nB} \left(K_{nk} \frac{\rho}{\rho_T} \right) \cos \left[nB\theta + \left(\frac{nBM^2}{\beta^2} - \mu_{nk} \right) z \right] \quad (9)$$

while the far-wake axial perturbation velocity is

$$u(r, \theta, z \rightarrow \infty) = \frac{wB}{2\pi U} \left\{ \frac{C}{\beta^2} - \Gamma(\rho) - \sum_{n=1}^{\infty} (-2)(-1)^n \times \chi_n(\rho) \cos(nB\zeta) \right\} + \frac{wB}{2\pi U} \sum_{n=1}^{\infty} \sum_{k=1}^{k_n^*} \left\{ \frac{(-1)^n h_{nk}}{\beta^2 \mu_{nk}} \times \left(\frac{nBM^2}{\beta^2} - \mu_{nk} \right) + (-1)^n (h_{nk} + \Gamma_{nk}) \frac{nBM^2 / \beta^2 - \mu_{nk}}{nB} \right\} \times R_{nB} \left(K_{nk} \frac{\rho}{\rho_T} \right) \cos \left[nB\theta + \left(\frac{nBM^2}{\beta^2} - \mu_{nk} \right) z \right] \quad (10)$$

As discussed in the previous section the terms involving the sums over k in the previous expressions represent acoustic radiation and vanish identically if $M_{rT} \leq 1$.

In either case, subsonic or transonic, if we consider the azimuthal average of v and u in the far wake we find simply

$$\langle v(r) \rangle_{\infty} = B\Gamma(\rho) / 2\pi r \quad (9a)$$

and

$$\langle u(r) \rangle_{\infty} = (\omega B / 2\pi U) [C / \beta^2 - \Gamma(\rho)] \quad (10a)$$

The latter quantity is the required (average) change in axial speed associated both with streamline displacement and with the change in pressure (and hence density) across the rotor. Note that $\langle u \rangle_{\infty}$ is not zero even in incompressible

flow ($\beta^2 = 1$) unless $\Gamma = \text{const}$, in which case $C = \Gamma$. This effect is due to streamline displacement.

Equation (9a), on the other hand, yields the familiar relationship between the circulation and the mean tangential velocity induced by the rotor. This particular result is general and is not limited by the linearizing approximations.

To first order the static pressure perturbation is given by

$$p = -\sigma_{\infty}(Uu + \omega r v)$$

and hence the average static pressure rise across the rotor is quite simple

$$\langle p \rangle_{\infty} = -\sigma_{\infty}[U^2(\omega B/2\pi U)C/\beta^2] \quad (11)$$

Note that this first-order quantity is independent of radius for any $\Gamma(r)$. However, "radial equilibrium"—satisfaction of the radial momentum balance, which requires a radial pressure gradient associated with $v(r, \theta, x)$ —plays an important role in second-order calculations. (Note that because of the convention we have used in defining $\Gamma(r)$, it is negative for a blade section which is doing work on the gas in duct coordinates.)

The static pressure rise across the rotor tends to be a strong function of the axial Mach number. In contrast, the average total pressure ratio across the rotor (in duct, rather than rotor, coordinates and to first-order in disturbance quantities) is given by

$$\frac{\langle p_0(r) \rangle_{\infty}}{\langle p_0 \rangle_{-\infty}} = 1 - \frac{\gamma M^2 \rho_T \Gamma(\rho)/UL_T}{1 + [(\gamma - 1)/2]M^2} \quad (12)$$

where we have introduced the blade spacing at the tips, $L_T = 2\pi r_T/B$. The total pressure rise is a weaker function of Mach number than is $\langle p \rangle_{\infty}$ and is independent of radius only for constant work design.

A first-order momentum balance across the rotor reveals that the axial and tangential components of the force on the blades are given by the classical formulas applied at each radius

$$F_{\theta}^{(1)} = -\sigma_{\infty}U\Gamma(r); \quad F_x^{(1)} = \sigma_{\infty}\omega r\Gamma(r) \quad (13)$$

The total torque delivered by the rotor to the fluid is, to first order,

$$\mathbf{T}^{(1)} = -\sigma_{\infty}UBr_T^2 \int_h^1 \eta d\eta \Gamma(\eta) \mathbf{e}_x \quad (14)$$

where \mathbf{e}_x is the unit vector in the axial direction. If we define the torque coefficient as $C_T = (\mathbf{T}^{(1)} \cdot \mathbf{e}_x)/\sigma_{\infty}U^2 r_T^3$ then

$$C_T = -\pi(1 - h^2)C/UL_T \quad (14a)$$

Eliminating C between Eqs. (11) and (14) we obtain the relationship between torque input and the static pressure rise across the rotor [here, $C_p \equiv \langle p \rangle_{\infty}/(\sigma_{\infty}U^2/2)$]

$$C_p = (2\rho_T/\beta^2)C_T/(1 - h^2) \quad (15)$$

Within the small-perturbation approximation of the present theory the mean turning angle δ induced by the rotor (viewed in rotor coordinates) is determined by $\phi_{\infty} \equiv (\phi - \delta) = \tan^{-1}[(\omega r + \langle v \rangle_{\infty})/(U + \langle u \rangle_{\infty})]$, which, according to Eqs. (9a) and (10a), yields

$$\delta = -(1/\eta)[\Gamma(\eta)/UL_T][1 - (C/\beta^2\Gamma)\rho^2/(1 + \rho^2)] \quad (16)$$

If $\Gamma = \text{const}$, so that $C = \Gamma$, this becomes

$$\delta = -C/\eta UL_T \beta^2 \cos^2 \phi(\rho)[1 - M^2/\cos^2 \phi(\rho)] \quad (16a)$$

Note that δ changes sign along the span if the relative Mach number $M/\cos \phi$ exceeds unity, even though the swirl [Eq. (9a)], sectional work, and circulation all remain of the same sign. This is an important effect of compressibility; it also reflects our assumption of isentropic flow, which excludes shock turning.

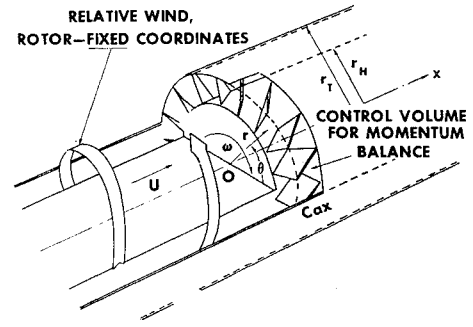


Fig. 1 Flow is steady in rotor coordinates. Relative unperturbed speed U_r is $(U^2 + \omega^2 r^2)^{1/2}$.

We now introduce the local two-dimensional lift coefficient of a blade section of chord $c(\eta)$

$$C_L(\eta) \equiv 2L(\eta)/\sigma_{\infty}U_r^2 c(\eta) = -2\Gamma(\eta)/U_r(\eta)c(\eta)$$

and its average defined by

$$\bar{C}_L \equiv \int_h^1 U_r(\eta)C_L(\eta)c(\eta)d\eta / \int_h^1 U_r(\eta)c(\eta)d\eta$$

Then, for example

$$\frac{C}{UL_T} = -\bar{C}_L \left\{ \frac{1}{1 - h^2} \int_h^1 \eta d\eta (1 + \eta^2 \rho_T^2)^{1/2} c(\eta) / L_T \right\}$$

where the term in braces is a geometrical factor depending on the hub-to-tip ratio, stagger angle, and solidity of the blading. In the particular case for which the axial projection, c_{ax} , of $c(\eta)$ is a constant, this becomes

$$\frac{C}{UL_T} = \frac{-\bar{C}_L[2(1 - h^2) + \rho_T^2(1 - h^4)]}{4(1 - h^2)} \frac{c_{ax}}{L_T}$$

and

$$C_T/\bar{C}_L = (\pi/4)[2(1 - h^2) + \rho_T^2(1 - h^4)]c_{ax}/L_T \quad (17)$$

The mean induced tangential velocity at each radius can also be expressed in terms of $C_L(\eta)$:

$$-\langle v \rangle_{\infty}/U = [(1 + \rho_T^2 \eta^2)^{1/2}/2][c(\eta)/\eta L_T]C_L(\eta) \quad (18)$$

The advantage of expressions such as Eqs. (17) and (18) is that they contain explicitly the geometrical properties of the cascade as well as the section lift coefficient, all quantities whose typical values are familiar or readily estimated.

IV. Second-Order Calculations—Power Required and Ideal Efficiency

In this Section we extend the results of the linear theory by using them to derive certain relationships correct to second order in first-order quantities. If we carry out an angular momentum balance across the rotor, using the control volume indicated in Fig. 1 and retaining terms of second order, we find the appropriate generalization of Eq. (14), giving the total (integrated) torque required to drive the rotor. The result is $\mathbf{T}^{(2)} \equiv T^{(2)}\mathbf{e}_x$, where

$$T^{(2)} = -\sigma_{\infty}U r_T^2 B \int_h^1 \eta d\eta \Gamma(\eta) - \sigma_{\infty}r_T^2 \int_0^{2\pi} d\theta \int_h^1 \eta d\eta \{ [(\beta^2 u^d - M^2 \rho v^d) r v^d]_{z=0} - [(\beta^2 u^u - M^2 \rho v^u) r v^u]_{z=0} \} \quad (19)$$

Here, $\delta_x \equiv \omega c_{ax}/U$, assumed independent of r for simplicity (see below).

The leading term in Eq. (19) will be recognized as being identical to the "first-order" result Eq. (14). The second-order contributions in Eq. (19) are obtained by using the

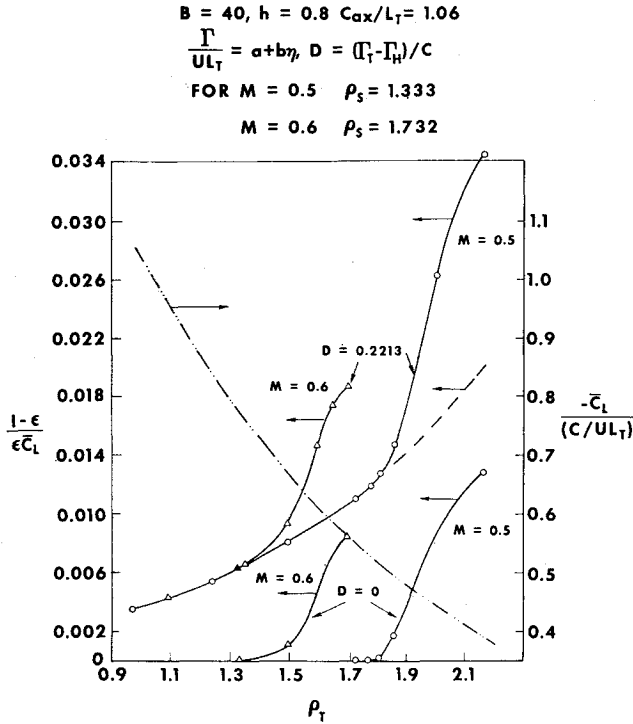


Fig. 2 Normalized ideal efficiency decrement.

first-order expression for the perturbation density in terms of u and v . [Only momentux flux terms appear in Eq. (19) although the flow in duct coordinates is unsteady. Equation (19) is nevertheless complete because the integral over the volume of the rate of change of angular momentum density vanishes identically.]

Ordinarily, a calculation of this kind would be subject to a "second-order error" since we have used the first-order expression for v in the leading term. However, as pointed out below Eq. (9a), the relation between

$$\int_0^{2\pi/B} d\theta v(r, \theta) r$$

and $\Gamma(r)$ is actually exact and hence the leading term in Eq. (19) is in fact correct to all orders.

This result can also be obtained independently through an energy balance (flux of enthalpy) which yields the power required, namely $\dot{W}^{(2)} = \omega T^{(2)}$.

The latter calculations, supporting Eq. (19), also imply "radial equilibrium," i.e., satisfaction of the radial momentum balance. It is not difficult to show that, consistent with Eq. (19),

$$(\partial h / \partial r)(z \rightarrow \infty) = v^2 / r \quad (20)$$

if $\Gamma = \text{const}$. In writing Eq. (20) we have used the Gibbs Equation and the fact that the flow is isentropic in the present model.

We wish to apply Eq. (19) both for subsonic and supersonic relative tip Mach numbers. In the latter case, as mentioned in the introduction, we must turn to lifting surface theory. The reason for this will become apparent below; it is related to the fact that the "wave drag" of an isolated supersonic vortex is undefined.

The lifting surface theory is constructed from the Green's function solution of Sec. II by distributing the bound vorticity (with its corresponding wakes) over helical surfaces of finite chord, $c(\eta)$. The local strength of the bound vorticity is $\gamma(\eta, \xi) d\xi / \cos \phi$, and

$$\int_0^{c_{ax}(\eta)} \frac{d\xi \gamma(\eta, \xi)}{\cos \phi} = \Gamma(\eta) \quad (21)$$

where $c_{ax} = c \cos \phi$. In the following we take a simplified version of the general theory in which $c_{ax} = \text{const}$ and $\gamma(\eta, \xi) = \Gamma(\eta) \cos \phi g(\xi)$ so that, from Eq. (21)

$$\int_0^{c_a} d\xi g(\xi) = 1$$

In the explicit calculations presented in Sec. V we simplify further, putting $g(\xi) = (c_{ax})^{-1}$. This is sufficient to demonstrate the effect of acoustic radiation on the power required; variations of $g(\xi)$ over the chord simply introduce additional radiation due to higher-order multipoles.

Proceeding in this way we compute $u^d(r, \theta, \delta_x)$, $v^d(r, \theta, \delta_x)$, $u^u(r, \theta, 0)$, $v^u(r, \theta, 0)$ and carry out the indicated operations in Eq. (19). Using the orthonormality of the radial and azimuthal eigenfunctions, we obtain

$$\begin{aligned}
 T^{(2)} = & -\sigma_{-\infty} U r_T^2 B \int_h^1 \eta d\eta \Gamma(\eta) + \\
 & \sigma_{-\infty} \frac{\omega B^2 r_T^2}{2\pi U} \int_h^1 \eta d\eta \left\{ \Gamma(\Gamma - C) + 2 \sum_{n=1}^{\infty} \chi_n^2(\rho) \right\} - \\
 & \sigma_{-\infty} \frac{\omega B^2 r_T^2}{4\pi U} \int_h^1 \eta d\eta \Gamma \sum_{k=1}^{\infty} \Gamma_{0k} R_0(K_{0k}\eta) e^{-\lambda_{0k}\delta_x} G_{0k}^d - \\
 & \sigma_{-\infty} \frac{\omega B^2 r_T^2}{2\pi U} \sum_{n=1}^{\infty} \sum_{k=1}^{\infty} \left((2h_{nk}^2 + h_{nk} \Gamma_{nk}) \times \right. \\
 & \left. \text{Re} \left\{ \exp \left[\left(\frac{inB}{\beta^2} - \lambda_{nk} \right) \delta_x \right] (G_{nk}^d) \right\} - h_{nk}(h_{nk} + \Gamma_{nk}) \frac{\beta^2}{nB} \times \right. \\
 & \left. \text{Re} \left\{ i\lambda_{nk} \exp \left[\left(\frac{inB}{\beta^2} - \lambda_{nk} \right) \delta_x \right] (G_{nk}^d) \right\} + \right. \\
 & \left. h_{nk}^2 \frac{nB}{\beta^2} \text{Re} \left\{ \left(\frac{i}{\lambda_{nk}} \exp \left[\left(\frac{inB}{\beta^2} - \lambda_{nk} \right) \delta_x \right] \right) (G_{nk}^d) \right\} \right) + \\
 & \sigma_{-\infty} \frac{\omega B^2 r_T^2}{4\pi U} \sum_{n=1}^{\infty} \sum_{k=1}^{k_n^*} \left\{ \left(\frac{h_{nk}^2 nB}{\beta^2 \mu_{nk}} + (h_{nk} + \Gamma_{nk})^2 \frac{\beta^2 \mu_{nk}}{nB} \right) \times \right. \\
 & \left. (|G_{nk}^d|^2 + |G_{nk}^u|^2) + 2h_{nk}(h_{nk} + \Gamma_{nk})(|G_{nk}^d|^2 - |G_{nk}^u|^2) \right\} + \\
 & \sigma_{-\infty} \frac{\omega B^2 r_T^2}{4\pi U} \sum_{n=1}^{\infty} \sum_{k=(k_n^*+1)}^{\infty} \{ 2h_{nk}(h_{nk} + \Gamma_{nk}) \times \\
 & (\exp[-2\lambda_{nk}\delta_x] |G_{nk}^d|^2 - |G_{nk}^u|^2) \} \quad (22)
 \end{aligned}$$

where $\text{Re}[\]$ indicates "real part." The "radiative terms," i.e., the power associated with acoustic radiation for supersonic tip Mach number, can be identified readily from the presence of the sum over k from 1 to k_n^* .

The quantities G_{nk}^d and G_{nk}^u are complex functions of the normalized chord, δ_x given by

$$G_{nk}^{u,d} = \frac{U}{\omega} \int_0^{\delta_x} dz g \left(\frac{Uz}{\omega} \right) \exp \left[-z \left(\frac{inB}{\beta^2} \pm \lambda_{nk} \right) \right]$$

For the particular case $g(\xi) = (c_{ax})^{-1}$ we have

$$G_{nk}^{u,d} = \frac{1 - \exp \left[-\delta_x \left(\frac{inB}{\beta^2} \pm \lambda_{nk} \right) \right]}{\delta_x \left(\frac{inB}{\beta^2} \pm \lambda_{nk} \right)} \quad (23)$$

The latter expressions were used in the explicit computations presented in Sec. V.

For constant work design, $\Gamma = \text{const} = C$, all the χ_n 's and h_{nk} 's vanish, and the Γ_{0k} 's are also identically zero. Hence, for constant work, the power required, $\omega T^{(2)} = \dot{W}^{(2)}$ reduces to

$$\begin{aligned}
 \dot{W}_{\Gamma=C^{(2)}} = & -\sigma_{-\infty} U r_T^2 \omega B (1 - h^2) C / 2 + \\
 & \sigma_{-\infty} \frac{\omega B^2 r_T^2}{4\pi U} \sum_{n=1}^{\infty} \sum_{k=1}^{k_n^*} \frac{\beta^2 \mu_{nk}}{nB} \Gamma_{nk}^2 (|G_{nk}^d|^2 + |G_{nk}^u|^2) \quad (22a)
 \end{aligned}$$

This result reveals that in the purely subsonic case, the leading term, which is the same as the first-order result (Eq. 14), is in fact correct to second order if $\Gamma = \text{const}$.

The reduced result (22a) also reveals the necessity of using lifting surface theory to obtain a meaningful result for the acoustic power radiated for $M_{rT} > 1$. It will be observed that as $\delta_z \rightarrow 0$, corresponding to the concentrated bound vortex case (or "lifting line"), all the G_{nk} 's $\rightarrow 1$. Hence, if we could take this limit, the expression Eq. (22) would be enormously simplified. However, as Eq. (22a) shows, this limit cannot be taken inside the sums, since (when $M_{rT} > 1$) the sum over the radiative terms would then diverge. The reader can easily convince himself of this by noting that as $n \rightarrow \infty$, $k_n^* \rightarrow \infty$ (if $M_{rT} > 1$) and $\mu_{nk} \rightarrow nB\beta^{-2}\rho_T^{-1}(M_{rT}^2 - 1)^{1/2}$. But

$$\sum_{k=1}^{\infty} \Gamma_{nk}^2 = \int_h^1 \eta d\eta \Gamma^2(\eta) \quad (24)$$

independent of n , and the subsequent sum over n [cf. (22a)] does not exist. (This is in analogy with the result for the wave drag of a lifting flat plate airfoil of chord c in supersonic flow, for which $D_{\text{wave}} \sim \Gamma^2/c$.) This difficulty does not arise in the subsonic case. By retaining finite chord, convergence is assured even in the mixed flow case.

A. Ideal Efficiency

At first glance, it would appear difficult to define a meaningful efficiency since no losses are directly accounted for in the theory.

We have seen however, that if $\Gamma \neq \text{const}$, a highly structured flow pattern appears downstream of the rotor, involving both concentrated free vorticity in the wakes and induced three-dimensional flow between them [cf. Eq. (4)]. In addition, if $M_{rT} > 1$, acoustic radiation occurs, which increases the required power input for a given $\Gamma(r)$.

We adopt the point of view that only an appropriate average of the flow energy can be expected to be diffused by a downstream stator and recovered as total pressure. The remaining flow energy should be expected to be dissipated (by mixing, say) or simply carried away by acoustic radiation.

To support this view, we have been able to show, by using an exact integral of the momentum equation, that the average over the flow annulus of the change across the rotor of the total specific enthalpy in duct coordinates is given by

$$\langle\langle (H_d)_\infty - (H_d)_{-\infty} \rangle\rangle = -\rho_T U^2 C / UL_T \quad (25)$$

regardless of the distribution over the span of $\Gamma(r)$ and independently of whether or not acoustic radiation occurs.

We are lead in this way to define an "equivalent constant work state" in which we replace the actual $\Gamma(\eta)$ by its average C . We then take the "ideal" or "useful" power required to be that corresponding to this equivalent smooth state, also omitting terms due to acoustic radiation. \dot{W}_{ideal} is then given by the leading term in Eq. (22a), correct to second order. This in turn leads to the definition of an "ideal efficiency" for any $\Gamma(r)$

$$\epsilon = \dot{W}_{\text{ideal}} / \dot{W}^{(2)} \equiv [-\sigma_{-\infty} U^3 \pi r_T^2 (1 - h^2) \rho_T C / UL_T] / \dot{W}^{(2)} \quad (26)$$

where $\dot{W}^{(2)} = \omega T^{(2)}$, obtained from Eq. (22).

We may write $\dot{W}^{(2)}$ in the form $\dot{W}^{(2)} = \dot{W}_{\text{ideal}} + \Delta \dot{W}^{(2)}$ where $\Delta \dot{W}^{(2)}$ represents the terms in (22) which are quadratic in Γ . Then

$$(1 - \epsilon) / \epsilon = + \Delta \dot{W}^{(2)} / \dot{W}_{\text{ideal}} \quad (27)$$

In the purely subsonic case, for which $\Delta \dot{W}^{(2)}$ is solely due to the energy in the wakes, a fair approximation for this ex-

pression is

$$\frac{1 - \epsilon}{\epsilon} = \frac{-\rho_T}{1 - h^2} \frac{UL_T}{C} \int_h^1 \eta d\eta \frac{\Gamma}{UL_T} \times \left[\frac{\Gamma - C}{UL_T} - 2 \sum_{n=1}^{\infty} \frac{\chi_n(\eta \rho_T)}{UL_T} \right] \quad (27a)$$

This result is obtained from Eq. (22) in the limit $\delta_z \rightarrow 0$, with $\rho_T < \rho_s$ so that all k_n^* are zero. In this limit all sums over k can be carried out exactly in Eq. (22). Note that in this case (subsonic flow) $\epsilon = 1$ if $\Gamma = \text{const}$, whether or not the approximate expression Eq. (27a) or the more exact version [Eq. (22) in Eq. (27)] is used. Although not exact, Eq. (27a) is a useful measure of the efficiency decrement associated with departure from constant work design. Since it no longer involves the radial eigenvalues and eigenfunctions, it is extremely handy for examining trends under variation of B or h (Sec. V).

Both Eq. (27) and Eq. (27a) are the ratio of terms quadratic in Γ to a term linear in Γ . For this reason we may normalize either expression with respect to any one of the linear quantities derived in Sec. III. The results in Section V are given in terms of the quantities

$$(1 - \epsilon) / \epsilon \bar{C}_L \text{ or } (1 - \epsilon) / \epsilon (-C / UL_T) \quad (28)$$

where \bar{C}_L is defined at the end of Sec. III. For our present purposes it is sufficient to use the expression for the special case $c_{ax} = \text{const}$, given immediately before Eq. (17).

The quantity (28) is independent of the magnitude of $\Gamma(r)$, depending only on the distribution of $\Gamma(r)$ over the span and geometrical properties of the rotor. Hence, it is also independent of Mach number in the subsonic range ($M_{rT} < 1$) except in so far as the distribution of $\Gamma(r)$ may change with M for a given rotor geometry. However, for $M_{rT} > 1$, when acoustic radiation occurs, an explicit Mach number dependence appears (Sec. V).

In the following section, we give results for the ideal efficiency decrement which illustrate both the effect of departure from constant work and the losses associated with acoustic radiation.

V. Discussion of Results

It was shown in Ref. 5 that the wake functions $\chi_n(\rho)$ may be evaluated in the approximate form

$$\chi_n(\eta \rho_T) \approx K'(\rho_T) I(\eta \rho_T) \int_h^1 \frac{I'(\eta' \rho_T)}{I'(\rho_T)} \eta' \frac{d\Gamma}{d\eta'} d\eta' + I'(h \rho_T) K(\eta \rho_T) \int_h^1 \frac{K'(\eta' \rho_T)}{K'(h \rho_T)} \eta' \frac{d\Gamma}{d\eta'} d\eta' - \int_\eta^1 I(\eta \rho_T) \times K'(\eta' \rho_T) \eta' \frac{d\Gamma}{d\eta'} d\eta' - \int_h^\eta K(\eta \rho_T) I'(\eta' \rho_T) \eta' \frac{d\Gamma}{d\eta'} d\eta' \quad (29)$$

Here η' is a dummy variable, but otherwise, the primes denote differentiation with respect to $\rho \equiv \eta \rho_T$ (cf. Sec. II A). In the following we also use the approximate expressions of Nicholson⁷ for the modified Bessel Functions.

As already noted, all results presented in this section are for a uniform chordwise loading $g(\xi) = (c_{ax})^{-1}$. For illustrative purposes, the radial loading distribution is taken to be of the simple form $\Gamma(\eta) \sim a + b\eta$. For $b \neq 0$, and any h , it is convenient to characterize the effect of deviation from uniform Γ in terms of the parameter $D \equiv [\Gamma(r_T) - \Gamma(r_H)] / C$.

As our first example, we choose a rotor with 40 blades, a hub-to-tip diameter ratio of 0.8, and a solidity, c_{ax}/L_T , of 1.06. For $B = 40$ and $h = 0.8$ the necessary radial eigenvalues, K_{nk} , and phase shifts,^{3,4} γ_{nk} , were worked out in Ref. 5. For this case, we illustrate the complete calculation, computing both the wake losses (for $D \neq 0$) and the losses due to acoustic radiation which occur as ρ_T exceeds ρ_s . In

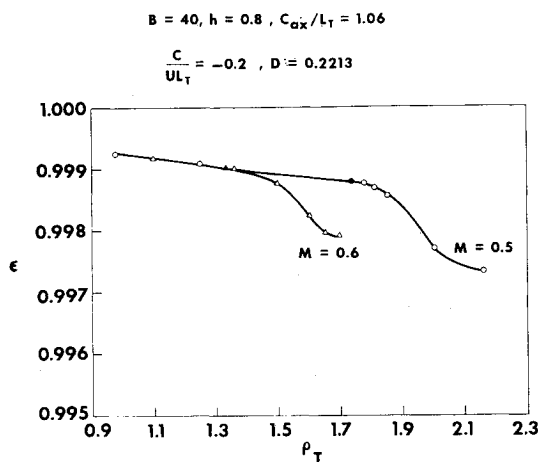


Fig. 3 Dependence of efficiency on tip speed.

the latter situation, if $D \neq 0$, resonant modes appear (see Secs. IIc and IV).

In the treatment of resonant modes, we assume here that a mode is "resonant" if its corresponding λ_{nk} or μ_{nk} is such that $|K_{nk}^2 - (nMB \rho_T)^2/\beta^2| \leq 0.002(nBM \rho_T)^2/\beta^2$. Thus, a mode may be "resonant" and yet remain essentially subsonic or supersonic (radiative) in character, depending on whether $K_{nk}^2 - (nMB \rho_T)^2/\beta^2$ is positive or negative. For resonant modes, modified values of λ_{nk} or μ_{nk} obtained by the method of Ref. 3 are used, assuming a Reynolds Number Ur_T/ν of 10^4 . To illustrate the effect of such modification, we note that for $B = 40$, $h = 0.8$, $M = 0.6$ and $\rho_T = 1.70$, $\mu_{4,6} = 35.24$, $\mu_{4,7} = 6.64$, and $\lambda_{4,8} = 39.63$. The (4,7) mode is resonant by the aforementioned criterion, and on the supersonic side of its exactly resonant condition. Modification of this mode accordingly yields $\mu_{4,7} = 18.92$.

As regards the computation of the second order torque from Eq. (22), we find that the series involving the χ_n 's converges very rapidly, and may be terminated after only 4 terms in n with better than 1% accuracy. Of the remaining series, those involving the radiative terms converge least rapidly. As a result, at subsonic relative tip Mach number, where the radiative terms are all zero, the first 4 or 5 in n will usually be enough for an accuracy of better than 1% at any k . Convergence in k is quite satisfactory. At supersonic relative tip Mach numbers the series involving radiative terms with coefficients of the type h_{nk}^2 or $h_{nk} \Gamma_{nk}$ converge in n rapidly enough for termination after about 5 or 6 terms. On the other hand, as we expect from Sec. IV, the series involving radiative terms with coefficients $\sim \Gamma_{nk}^2$ [cf. Eq. (22a)] converges essentially as n^{-2} at fixed k . From the well-known

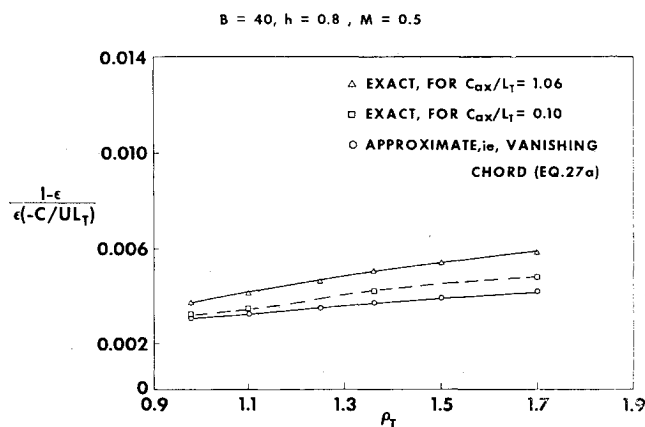
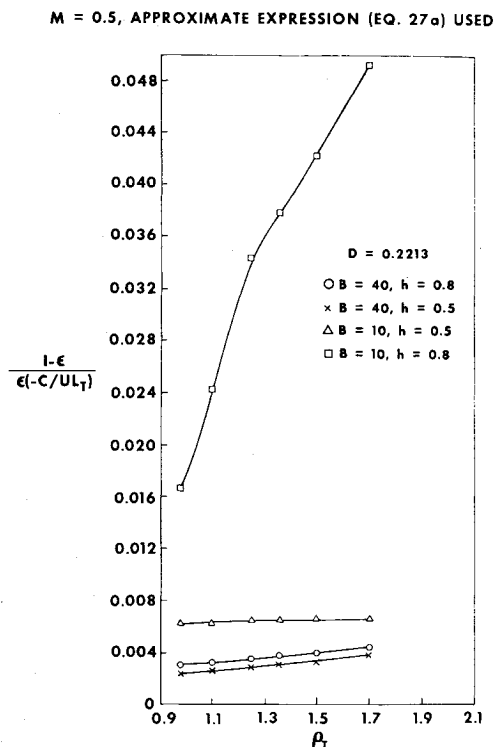
Fig. 4 Effect of solidity on calculated wake losses ($\rho_T < \rho_s$).

Fig. 5 Effect of hub-tip ratio and number of blades.

result

$$\sum_{n=1}^{\infty} \frac{1}{n^2} = \frac{\pi^2}{6}$$

we can estimate that termination of this particular series after 10 terms yields a maximum error of approximately 6% at any k . The actual error, because of the presence of the cosine terms with $\delta_x \neq 0$ (Sec. IV), is less because of compensating effects among the various terms. Moreover, after summation over k , the net error is believed to be further reduced since the error itself may oscillate in sign as k is increased. Although the convergence of this series could be improved by a variety of techniques, we believe that our present direct computations, in which we terminate the sums over n after 10 terms are inadequate to illustrate the desired results.

The ideal efficiencies for $B = 40$ and $h = 0.8$ are presented in Fig. 2 as a function of the dimensionless tip speed, ρ_T , for $D = 0$ and 0.2213, and for $M = 0.5$ and 0.6. For $M = 0.5$, the relative flow at the tip becomes supersonic at a value of $\rho_T = \rho_s = 1.732$. This point is identified by the shaded circles in Figs. 3 and 4. The corresponding point for $M = 0.6$ is at $\rho_T = 1.333$ and is identified by the shaded triangles. For a given value of D , the ideal efficiency decrement, normalized to \bar{C}_L , is independent of M , as long as $\rho_T < \rho_s(M)$. The losses in this region are entirely due to wake mixing, and are zero for constant work flow, i.e., $D = 0$. These losses may be regarded as being associated with the "induced drag" of the blades.⁵ The dashed curve in Fig. 2 is an extension of these "induced-drag losses" to transonic values of ρ_T , and is obtained by omitting the radiative terms from the second order torque. The build up of wave energy losses for $\rho_T > \rho_s(M)$ is shown by the rapid departure of the solid curves from this "base-curve." For $D = 0$, the only losses are due to acoustic radiation, and the base-curve here is simply the zero-loss axis.

To understand the nature of the build up of wave-losses, it should be noted that as ρ_T increases, k_n^* increases for fixed n , and approaches infinity as $n \rightarrow \infty$. Thus, increasing ρ_T causes an increasingly larger number of modes to undergo a transition from subsonic to supersonic in character, and

hence, to become radiative. Moreover, since for each n the dominant modes are those corresponding to low values of k , and are the first to become radiative, it would be expected that the acoustic energy initially builds up very rapidly once ρ_T becomes greater than $\rho_s(M)$, and then gradually levels out. These phenomena are illustrated by Fig. 2.

Since we have normalized the efficiency decrement by \bar{C}_L , which is a function of ρ_T , we have also shown on Fig. 2 the dependence of this quantity on ρ_T . Thus, for specified values M and D , we can also obtain the variation of the efficiency with ρ_T for a given value of C/UL_T . The magnitude of C/UL_T is, of course, restricted by the need for consistency with the linearizing assumptions of the analysis. Thus, for example, if we limit the total pressure ratio across the rotor to values less than 1.2, $|C/UL_T|$ would be typically about 0.3 or less. For illustration, we have plotted in Fig. 3 the variation of the ideal efficiency with ρ_T for $C/UL_T = -0.2$ and $D = 0.2213$. We see here that the efficiency decreases almost linearly with ρ_T until the rotor becomes transonic, after which it drops rather sharply, tending to level out at a value depending on the axial Mach number.

The terminal value of ρ_T used in these calculation corresponds to a tip relative Mach number of 1.19 for $M = 0.5$ and 1.183 for $M = 0.6$. At these Mach numbers, with $B = 40$ and $h = 0.8$, the reduction in efficiency is of the order of $\frac{2}{10}$ to $\frac{3}{10}$ of 1%. The smallness of these numbers, even for 20% departure from constant work, indicate that "induced-drag losses" probably do not importantly degrade the compressor performance of a rotor, if it has a large number of blades and large hub-to-tip ratio. However, these results are quite sensitive to the latter two parameters, and it is of interest to investigate their effect.

For this purpose the approximate expression Eq. (27a), in which all sums over k have been performed, is extremely useful to a quick survey of the effects of B and h . To demonstrate its usefulness, we compare in Fig. 4 the exact result for $(1 - \epsilon)/\epsilon$, computed from Eq. (22) with $\rho_T < \rho_s$, with the approximate result (27a) for $B = 40$ and $h = 0.8$. In Fig. 4, the efficiency decrement is normalized with respect to $-C/UL_T$, so the parameter c_{ax}/L_T enters only through δ_x in Eq. (22). The exact result is shown to approach Eq. (27a) as c_{ax}/L_T decreases, and in any case exhibits the same trend with ρ_T even for $c_{ax}/L_T = 1.06$.

In Fig. 5 results for the efficiency decrement obtained from Eq. (27a) are shown as a function of ρ_T for $B = 40$, with $h = 0.8$ and $h = 0.5$, and for $B = 10$ with the same two values of h . In each case the deviation from constant work is held

constant at $D = 0.2213$. The following trends are immediately apparent. At fixed B and D , the wake losses decrease with decreasing hub-to-tip ratio. This is to be expected, since the nonuniformity in Γ is spread over a larger blade span. On the other hand, at fixed h the losses increase substantially for rotors with a fewer number of blades, an effect which is due to the heavier loading of the individual blades and the increased "coarseness" of the wake flow behind the blade row.

We note from Fig. 5 that for $B = 10$ and $h = 0.5$ a deviation of 20% from constant work leads to fairly substantial wake losses. These, combined with radiative losses in the transonic regime, may then lead to an efficiency decrement for such a rotor of close to 0.5% if a total pressure ratio of about 1.2 is assumed. For $B = 10$ and $h = 0.8$ the wake losses, as indicated in Fig. 5, are even larger and become surprisingly sensitive to ρ_T . However, this particular combination of B and h represents a rather unlikely compressor configuration.

Finally, we observe that the efficiency decrement described here increases linearly with increasing rotor loading. Although the present linearized theory cannot be expected to be accurate for total pressure ratios much in excess of 1.2, it should give a reliable indication both of the trends and the correct order of magnitude of the losses treated here, even for higher loadings.

References

- ¹ Reissner, H., "On the Vortex Theory of the Screw Propeller," *Journal of the Aeronautical Sciences*, Vol. 5, No. 1, Nov. 1937, pp. 1-7.
- ² Davidson, R. E., "Linearized Potential Theory of Propeller Induction in a Compressible Flow," TN 2983, 1953, NACA.
- ³ McCune, J. E., "The Transonic Flow Field of an Axial Compressor Blade Row," *Journal of the Aerospace Sciences*, Vol. 25, No. 10, Oct. 1958, pp. 616-626.
- ⁴ McCune, J. E., "Three-Dimensional Theory of Axial Compressor Blade Rows—Application to Subsonic and Supersonic Flows," *Journal of the Aerospace Sciences*, Vol. 25, No. 9, Sept. 1958, pp. 544-560.
- ⁵ Okurounmu, O., "Wave Drag in Transonic Axial Compressors," Sc. D. thesis, Nov. 1967, Dept. of Mechanical Engineering, Massachusetts Institute of Technology.
- ⁶ Watson, G. N., *A Treatise on the Theory of Bessel Functions*, 2nd ed., MacMillan New York, 1944.
- ⁷ Nicholson, J. W., "The Approximate Calculation of Bessel Functions of Imaginary Argument," *Philosophical Magazine*, Ser. 6, Vol. 20, pp. 938-943.